Forensic Science International 294 (2019) 21–26

Contents lists available at ScienceDirect

Forensic Science International

journal homepage: www.elsevier.com/locate/forsciint

Forensic personal identification utilizing part-to-part comparison of CT-derived 3D lumbar models

Summer J. Decker*, Jonathan M. Ford

Department of Radiology, University of South Florida Morsani College of Medicine, 2 Tampa General Circle, STC7033, Tampa, Florida, 33606, USA

ARTICLE INFO

Article history:
Received 18 June 2018
Received in revised form 11 October 2018
Accepted 17 October 2018
Available online 29 October 2018

Keywords:
Forensics
Radiology
Post-mortem computed tomography
3D
Personal identification
Part-to-part comparison

ABSTRACT

The objective of this project was to document the efficacy of part-to-part comparison of computed tomography (CT)-derived three-dimensional (3D) models of the lumbar spine in forensic personal identification. By testing the methodology, this study aimed to provide a new technique of quantifiable (through a percent match) positive identification that meets the explicit requirements of the Daubert ruling and the challenges set forth in the 2009 NAS report. Ante-mortem (AM) and simulated post-mortem (PM) models of the lumbar vertebrae (L1–L5) for 30 unique individuals were compared via part comparison analyses. The threshold of ±0.5 mm with at least a 90% match was considered a positive identification. Using this threshold, the part comparison results had a perfect identification rate with no false positives and no false negative matches. A ROC curve was generated with a score of 1, signifying a "perfect" sensitivity and specificity, at a cut-off value of 65.5%. On average positive IDs had a 94.7% percent match within the established threshold, while negative IDs had an average of 21.4%. In looking at the impact of different components of the biological profile, age and sex of the unknown individual played a minimal role in the percent match for both a positive and a negative ID. Lumbar level also played a minor role in in both the positive and negative percent match. The real-world application of 3D part-to-part comparison on AM and simulated PM scans demonstrate the potential usefulness of this technology in forensic identification.

1. Introduction

Emerging technologies are allowing for the development of new applications to address forensic concerns. One of the critical components of any forensic investigation is the identification of the deceased. As the current population in the US and world has increasing access to advanced medical imaging, it is presenting an opportunity to utilize these medical records as a source for personal identification. This study attempts to demonstrate the potential utility of ante-mortem (AM) and post-mortem (PM) image matching of the lumbar vertebrae through part-to-part comparison for forensic identification.

1.1. Forensic identification

Once the body of an unknown person is discovered, practitioners are tasked with identifying the human remains. Natural processes such as decomposition [1], lengthy submersion in water [2], burning [3,4] or even animal activity [5] can make identification a challenge. The intentional obscuration of the deceased's identity by means of decapitation, disfigurement, or dismemberment is also a potential complicating factor. Furthermore the manner of death, like catastrophic damage from a mass disaster, trauma from vehicle crashes, plane crashes or terrorist attacks [6,7] also destroy identifiers. In the event of a bombing or mass disaster, head injuries occur more frequently than would be predicted based on its 12% body surface area [8]. Once the biological profile is established, the remains are compared against suspected matches of known missing persons. DNA matching, comparison of dental records or radiographic matching [9,10] are all methods of establishing an identity. These methods all must meet the legal standards for forensic evidence in court as set forth in the *Daubert* ruling [11] based on the uniqueness proposition. The validity of uniqueness has been questioned recently with the release of the 2009 National Academy of Sciences report [12] which directly mandates the field to adequately "establish the uniqueness of marks or features".

* Corresponding author.
E-mail addresses: sdecker@health.usf.edu (S.J. Decker), jford@health.usf.edu (J.M. Ford).

https://doi.org/10.1016/j.forsciint.2018.10.018
0379-0738/

1.2. Forensic imaging

The use of post-mortem CT (PMCT) has quickly gained importance in the forensic field. The technology has introduced novel means of analysis and applications to forensic questions such as cause of death [13], identification of foreign bodies [14], incident reconstruction [15], and victim identification [6]. Previous literature has demonstrated that the frontal sinuses are as unique as fingerprints and a multitude of studies are published supporting this idea [16–23]. In addition to teeth [24], the skull has several features such as the mastoid air cells [19,25] and the paranasal sinuses [16–23,26] have been successfully used for forensic identifications. Other regions of the body used for radiographic identification include clavicles [27,28], costal cartilage [26,29], sternum [30,31], hip [21,32], vertebral features [30,32,33] as well as the extremities [19,26] to name a few. One limitation of radiographic identification is the inherent subjectivity of the process. Most positive identifications from medical image data simply involve the process of identifying key anatomical features on an AM image then comparing those against the outlines or other features that visually match the PM images. More recently, efforts have been made to objectively quantify AM and PM images in both dental [34] and radiographic areas [16,22,28].

In practice, the decision as to which anatomical structures to use in identification comparisons is limited by what type of AM scan an individual has had and of what region, as well as what portion of the remains is available for PM scanning. Over the five-year sample period of 2012–2016, the breakdown of the regions of the body that were scanned at [Tampa General Hospital] (a Level 1 trauma center that services a diverse metropolitan area of well over 3 million people) consisted of 72,607 CT scans per year with 29% being head scans and 45% capturing the abdomen and pelvis. Considering the increased likelihood that the torso would survive a traumatic event, the higher rates of clinical abdominal and pelvic scans, as well as documented previous successes using vertebral features, it is for these reasons that this study chose to examine the lumbar vertebrae as a potential source of anatomically distinct structures to be used for positive human identification.

1.3. Part-to-part analysis

3D part-to-part comparison, part comparison, or 3D part inspection is a commonly used tool in computer aided design (CAD) and the manufacturing industry. The primary objective of part comparison is to test and guarantee the geometric accuracy of a product by comparing a sample 3D scan, against a "gold standard" in the form of an original prototype or original 3D CAD model [35,36]. Once a sample part is scanned and successfully digitized, an algorithm calculates the distance between that sample part and the target part. Every point of the sample part is compared against every point of the target part to find the nearest point relative to itself. Once the nearest point is found, the distance between every target point and sample point is calculated. This allows for the creation of color-map and a histogram showing the overall distance or differences between the two parts. The output from the analysis is a percentage match. The threshold of what an acceptable distance is chosen by the user. While gold standard in mechanical manufacturing, part-to-part comparison has recently been introduced to medicine [37,38]. A forensic pilot study utilized 20 3D reconstructed frontal sinuses from CT and used superimposition to achieve a 100% match in surface anatomy as a measurement of a positive identification [22]. Another recent case that has already utilized 2D and 3D superimposition to visually identify the partial remains of a murdered individual [23].

Medical imaging like CT is allowing for the 3D virtual reconstruction and analysis of relevant anatomy. The ability to computer model and analyze human remains provides the opportunity for the use of more robust analyses like part-to-part comparison. The primary aim of this project was to test and validate a new quantifiable method of radiologic comparison for positive personal identification using CT derived 3D computer models of the lumbar vertebrae (L1–L5) through superimposition and part-to-part comparison.

2. Materials and methods

2.1. Samples

A total 30 individual clinical CT scans of 15 males (43.5 ± 14.6 years) and 15 females (43.1 ± 15.1 years) were selected at random under IRB approval from the [USF Department of Radiology's] medical image research database which currently stores all clinical scans from 2009 to present. To account for any potential influence of sex or age, 15 males and 15 females for each decade of life between ages 20 through age 66 were selected at random. The sample consisted of a US population, with no record of ancestry. Only CT scan series that captured all 5 lumbar vertebrae were utilized. Any individuals exhibiting metallic surgical implants or unhealed fractures as well as any individuals that have the anatomic variation of 4 or 6 lumbar vertebrae were excluded from this study. This dataset does not include any PM scans, only those clinically ordered diagnostic imaging captured as part of the patient's standard of clinical care and therefore no individuals were subjected to any radiation for research purposes. None of the selected patient scans had been performed for lumbar issues or had a history back pathology. All scans were acquired on a GE LightSpeed VCT 64-slice scanner (General Electric, Chicago, Illinois, United States) at a 1.25 mm slice-thickness, kVp 120, Standard Filter, with mA and FOV size being variable depending on patient size.

This initial set of scans served as the AM scans for the purposes of this study. To simulate PM scans, each image dataset was resliced to generate a new but different dataset of the same individual. Despite best efforts, it is impossible to place a specimen in the exact orientation on a CT scanner's gantry and human remains are not often flexible enough to adjust body position. Therefore, in practice there will inherently be different planes of capture when comparing actual AM and PM scans. Slice-thickness, capture planes and other scanner parameters have been shown to effect the end result of 3D models generated from medical imaging. 3D models derived from medical scanning can be shortened, elongated or have completely missing anatomical geometries depending on these parameters [39–42]. By reslicing the AM scans, this process created entirely new datasets with different body orientations to mimic a scan captured at a different time i.e. a PM scan. The initial reslicing and the subsequent 3D modeling for both AM and simulated PM scans was conducted in the *Mimics Innovation Suite 20.0* (Materialise NV, Leuven, Belgium). For the simulated PM scans, the AM DICOM files were resliced using the reslice-tool where the entire image volume was randomly rotated along the central axis $\pm 3^{\circ}$ in addition to having the z-axis shifted $\pm 10^{\circ}$ in either the x or y (or both) directions. The new image volume was generated using the same slice-thickness of the original capture scan. A graphical example of the reslicing process can be seen in Fig. 1. An image showing an AM and PM reconstruction of the same vertebra can be seen in Fig. 2.

2.2. 3D modeling

Both AM and the simulated PM scans were given the same modeling treatment. All osseous material was captured utilizing the threshold of 226-3071 Hounsfield units. Additional hand segmentation was conducted as necessary on individuals whose

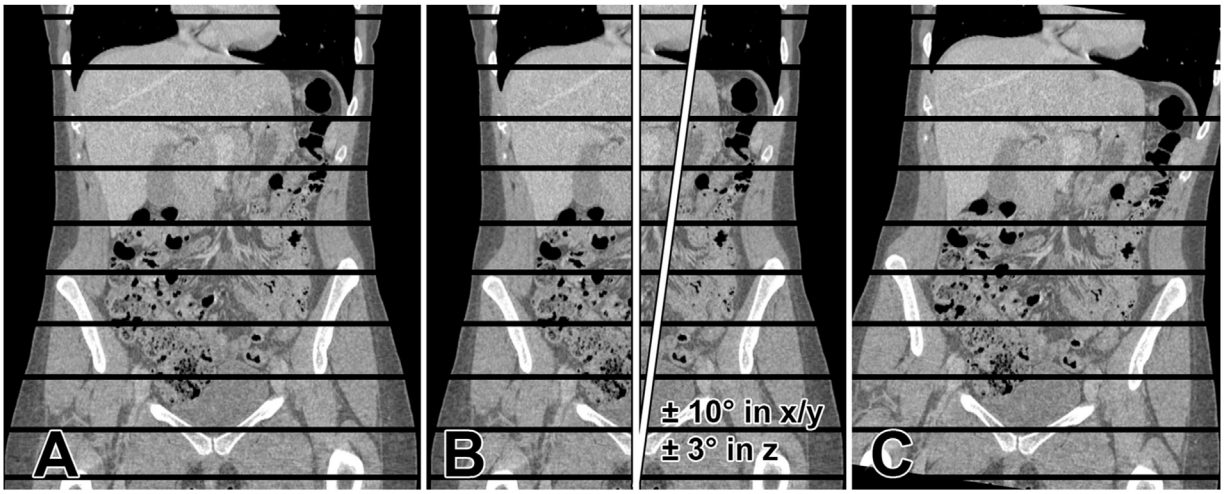

Fig. 1. Reslicing example: (A) original abdominopelvic scan, (B) resliced angle parameters altering the axis, & (C) resliced scan.

bone mineralization levels do not meet this threshold. Each lumbar vertebra was isolated from its immediate superior and inferior vertebrae via hand segmentation. Each lumbar was then made a solid structure to account for any variation in internal density from the trabecular bone. After each lumbar model was constructed, it was exported as a separate stereolithographic (STL) file. Each STL file was imported into the software package *3-matic*, also from Materialise NV, for model clean up, post-processing, and analysis. All noise shells were removed from the model. Each model was wrapped with a gap closing distance of 0.5 mm and a smallest detail threshold of 0.25 mm.

The 30 simulated PM scans served as a database of "unknown" individuals. The AM scans acted as the data set of known individuals. The lumbar vertebrae from the PM scans were labeled as L1JDoe1, L2JDoe1, L1JDoe3, and so forth. Only one person conducted the coding of the PM scans to ensure the study was properly blinded. Once all lumbar models were correctly coded, they were then provided to the study researchers to serve as targets for the "unknown" PM lumbar sample.

2.3. Part-to-part comparison

A part-to-part comparison analysis was conducted on every lumbar vertebra for every J.Doe using the part comparison analysis tool in *3-Matic*. Using the L1 scenario as an example, the target JDoe1 L1 vertebrae STL was imported into *3-Matic*. All 30 L1 vertebrae of "known" individuals' STLs were imported as well. Each "known" L1 vertebra was aligned to the target unknown L1 via point registration. Point registration was conducted by placing 9 landmark points on both the target and the test structure. The purpose of this initial landmark-based registration is to get the geometry of the unknown vertebra within close alignment with the target geometry. After an initial point registration, the alignment was further refined with a global registration. Then a global registration takes the all the vertexes of both geometries and uses them to calculate the best fit of the two objects. This preliminary landmark-based registration and subsequent global registration ensures that the proper alignment between the geometries is achieved and takes in to account any variations from landmark positioning. A list of landmarks can be seen in Table 1. These landmarks are also graphically depicted in Fig. 3.

Once this registration process was completed the actual part comparison was performed. The threshold of ± 0.5 mm with at least a 90% match was considered a positive identification. This $\sim$1 mm range was selected as most current clinical CT scanners can not reliably detect objects less than 0.6 mm as they have an in-plane spatial resolution of $\sim$0.3 mm and slice-thickness around 0.6 mm [41]. The percent match for

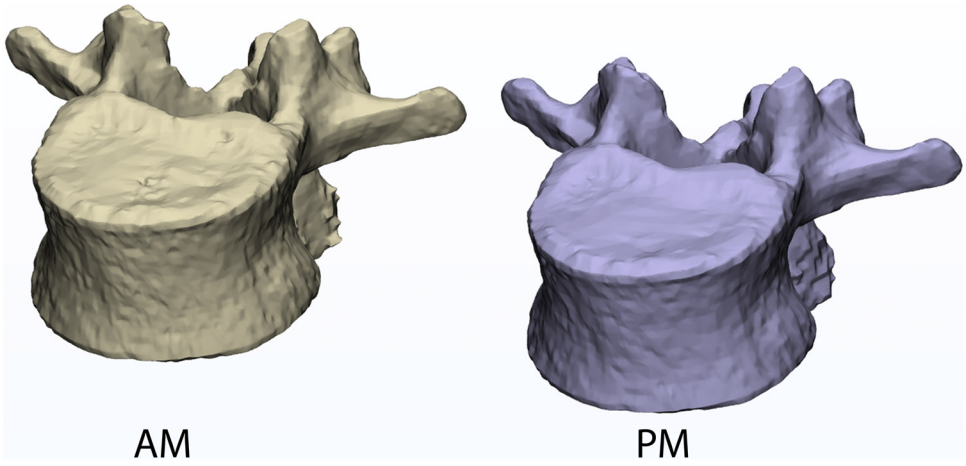

Fig. 2. Representative ante-mortem and post-mortem reconstruction of the same vertebra.

Table 1
Landmarks used in point registration.

Landmark	Abbreviation	Definition
Superior anterior endplate	SAE	Superior anterior most point along the sagittal plane of the vertebral body
Inferior anterior endplate	IAE	Inferior anterior most point along the sagittal plane of the vertebral body
Spinous process	SP	Most posterior point of the spinous process
Left transverse process	LTP	Left most point of the left transverse process
Right transverse process	RTP	Right most point of the right transverse process
Left superior articular process	LSAP	Most superior point of the left articular process
Right superior articular process	RSAP	Most superior point of the right articular process
Left inferior articular process	LIAP	Most inferior point of the left articular process
Right inferior articular process	RIAP	Most inferior point of the right articular process

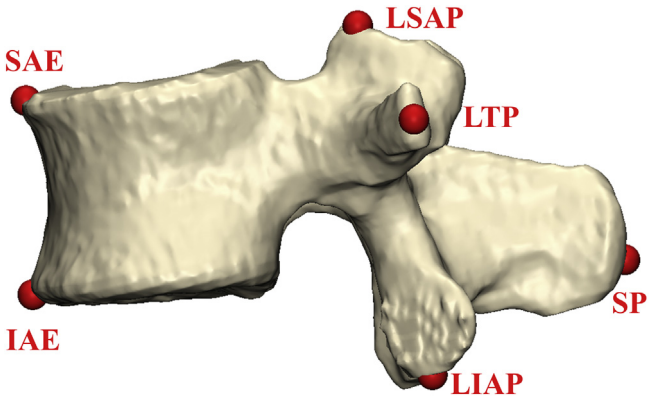

Fig. 3. Landmarks used in point registration.

every attempt was recorded to determine the average percent match for both a non-identification and a positive identification. A representative part-to-part comparison can be seen in Fig. 4. This process was conducted for every lumbar vertebra (L1–L5) for each of the 30 individuals.

2.4. Statistical analysis

All statistics were conducted using *SPSS 25* software (IBM). The goal of the following analyses was to quantify the range of variation among lumbar vertebra and the average measured unique geometry as defined by the percent match from the part-to-part analysis. The average percent match for every positive identification and average percent match for every non-match or non-identification was collected.

The positive identification and non-match results were broken down by vertebral level, age and sex. Statistical analyses comparing positive identifications and non-matches with respect to sex was conducted using independent t-test. Analyses with respect to age utilized a Pearson's correlation. A one-way ANOVA comparing the positive and negative match results was utilized on vertebral level with a follow up Tukey's post-hoc test to evaluate differences between vertebral levels. Anything with a p-value less than 0.05 was considered significant. A ROC curve was also generated testing sensitivity and specificity.

3. Results

The part comparison results yielded a 100% match with no false positives and no false negative matches. Positive identifications

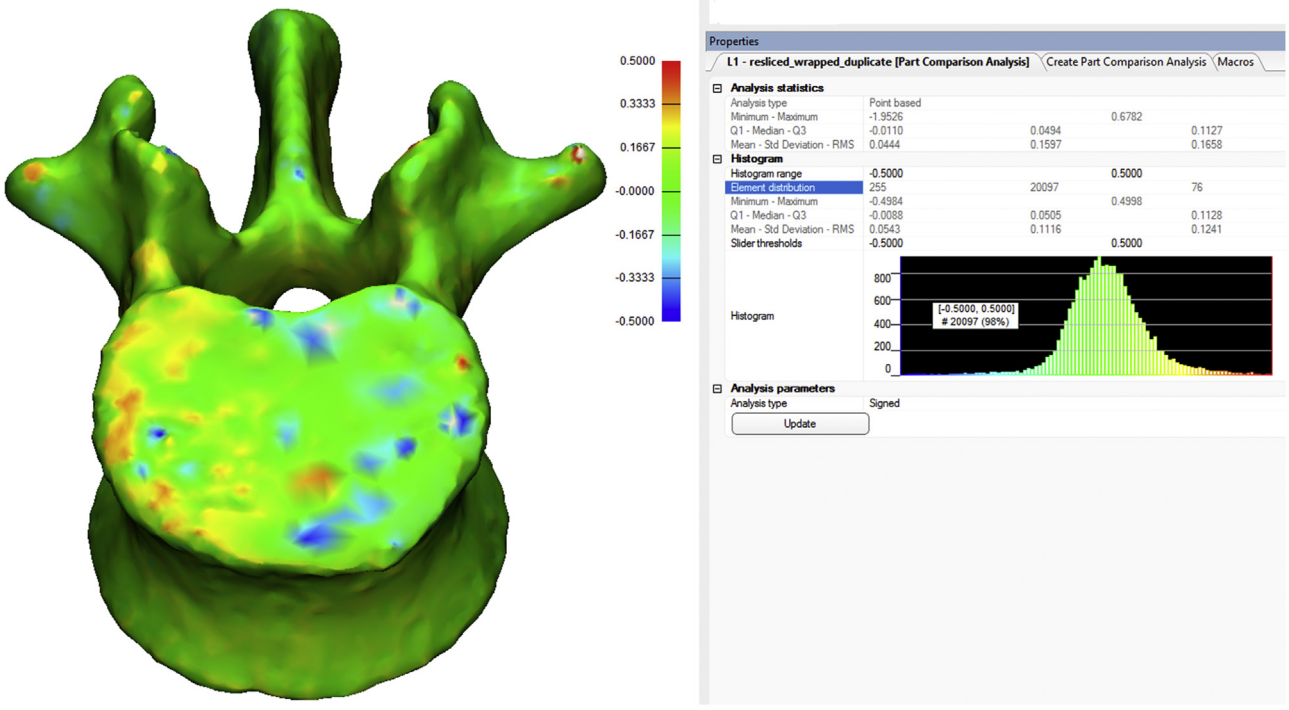

Fig. 4. Example part-to-part comparison analysis of L1 vertebra.

were above our 90% at ±0.5 mm agreement threshold with an average percent match of 94.7% ± 2.7%. Negative matches or non-identifications had an average percent match of 21.4% ± 8.0%. Additionally, a ROC curve was generated comparing the percent match values of a positive match and a negative match. The analysis returned with a score of 1, signifying a "perfect" sensitivity and specificity, with a cut-off value of 65.5%. An individual breakdown based on vertebral level can be seen in Table 2.

Despite the 100% success match rate in the initial findings. Any potential influence of sex, age or lumbar level were also examined. An independent t-test was run and there was no statistical difference between negative percent match for males (21.3% ± 7.98%) and females (21.6% ± 7.93%) with respect to a positive identification $p = 0.198$. However, there was a statistical difference between percent match for males (94.2% ± 2.6%) and females (95.2% ± 2.8%) with respect to a positive match; a statistically significant increase of 1.0%, $p = 0.023$.

A Pearson's correlation was run to assess the relationship between age and both positive matches and non-matches. There was a weak negative correlation to a person's age and positive percent match ($r = -0.274$, $n = 150$, $p = 0.001$). There was no significant correlation to an individual's age and the non-identification percent match ($r = 0.003$, $n = 4350$, $p = 0.854$).

There was a statistically significant difference between positive percent match and the relative vertebral level as determined by a one-way ANOVA ($F(4, 145) = 3.301$, $p = 0.013$). However, a Tukey post hoc test revealed that the only statistical difference was between L3 and L4 ($p = 0.022$). There was a statistically significant difference between negative percent match and the relative vertebral level as determined by a one-way ANOVA ($F(4, 4345) = 15.364$, $p > 0.001$). A Tukey post hoc test revealed that the percent negative match for L1, L2 and L3 were statistically higher, with L3 and L4 overlapping and L5 being statistically lower, $p > 0.05$.

4. Discussion

The aim of this study was to test if CT-derived 3D anatomical features, in our case the lumbar vertebrae (L1–L5), could be used as a means of personal identification using part comparison. This initial test was a success with a100% match rate implying the lumbar vertebra are anatomically distinct enough for personal identification. This anatomical uniqueness is further reinforced by the large disparity between the average "positive" match (94.7%) versus the average non-match (21.4%). In fact, the highest value for a non-match was 41%. To date there are no false positives, or false negatives. A ROC curve was generated with a score of 1, signifying a "perfect" sensitivity and specificity, at a cut-off value of 65.5%. At the onset of this study, the authors chose the threshold of 90% agreement within ±0.5 mm as the value needed for a positive identification. These initial findings show that a lower percentage threshold for establishing a positive identification may be possible.

Results pertaining to sex and age suggest that demographic information does not play a great role in personal identification when using part comparison. There was no statistical difference between males and females with respect to a negative match value. While there was a statistical difference between males and females with respect to a positive match value, the match value for females was only 1% higher than males. These results may be statistically significant but would not be considered significant in practice clinically or forensically. Additionally, there was a weak negative correlation, with a low R-score ($R = -0.274$, $p = 0.001$), to a positive percent match and age, signifying that older individuals may have slightly lower matching percentages on a positive identification. This slight decrease in positive percent match with respect to age may be on account that smaller anatomic age-related details, such as osteophytes, vertebral lipping, etc., may be lost between scans.

Furthermore, there is no clear advantage or disadvantage regarding lumbar vertebral level. The ANOVA based on vertebral level did identify some statistical differences. This difference between the upper (L1 and L3) and lower (L4 and L5) vertebrae may be on account of the natural size disparity between more superior and inferior lumbar vertebrae. The fact that L3 was not statistically different from either group and is acting as an "in between" vertebra further supports this idea. Ultimately, every vertebral level still successfully identified the unknown individuals ranging from a 90% to 100% match within ±0.5 mm.

While these initial results are promising, this method has yet to be attempted on a large-scale sample or another part of the body. The fundamental assumption however is that humans are anatomically unique enough to make a successful identifying match. Additionally, not all anatomical features are equal when it comes to usefulness in identification. Narrowing down a potential region requires one to consider not only the potential for its "survival" in traumatic injury as previous discussed, but also genetic and environmental factors which dictate and influence the way an individual develops and ages. One study showed that at least 44% of health young males have some identifiable anomaly of the lumbar spine [43]. While vertebrae do change with age, this change, when documented, provides additional unique structures to assist in the identification. While degenerative changes are contrary to the idea of stable identification markers, it should be noted that these changes are unidirectional and often well-documented. Any medical or surgical interventions to address spinal degenerative issues would be thoroughly imaged and have documented anatomy over time. Depending on the time since scan with the AM and PM scans, certain changes of the vertebra would not rule out a probable or positive identification. Future longitudinal studies should be undertaken examining how much time can elapse between AM and PM scans before significant changes occur that might hinder a positive identification. Furthermore, as the PM scans for this study were simulated additional testing must be performed on bona fide PMCTs to move this research beyond pilot status. The real-world application of 3D part-to-part comparison on actual AM and PM scans will demonstrate the usefulness of this technology in personal identification while also meeting the explicit requirements of Daubert ruling and demands of the NAS report.

As a scientific discipline, we must improve over current more subjective methods. Ordinal, scored and scaled data can now be

Table 2
Percent match.

Vertebral level	Average positive percent match	Average negative percent match
L1	95.3%	22.2%
L2	94.2%	22.4%
L3	95.9%	21.8%
L4	93.8%	21.1%
L5	94.2%	19.8%
Average	94.7%	21.4%

quantified by digitally capturing a specimen's actual 3D geometry for analysis. By doing so, 3D anatomical data is providing a direct increase in accuracy over traditional non-metric and more subjective methods. The use of 3D analyses is a natural progression because, after all, the human body is a complex and three-dimensional form. If these results continue in a larger sample, part-comparison based identification may become a viable quantifiable tool for personal identification on par with dental identification and fingerprints to aid in narrowing down an individual before DNA confirmation matching. The methods proposed in this project will be reproducible with reported accuracy and error rates and thereby present practitioners with a validated new technology to add to their human identification toolkit.

References

[1] N. Zanjad, H. Godbole, X-Ray examination–A good tool for identification in decomposed body: a case report, J. Indian Acad. Forensic Med. 29 (4) (2007) 92–93.
[2] K. Crainic, F. Paraire, M. Leterreux, M. Durigon, P. De Mazancourt, Skeletal remains presumed submerged in water for three years identified using PCR-STR analysis, J. Forensic Sci. 47 (5) (2002) 1–3.
[3] F. Dedouit, N. Telmon, R. Costagliola, P. Otal, F. Joffre, D. Rougé, Virtual anthropology and forensic identification: report of one case, Forensic Sci. Int. 173 (2) (2007) 182–187.
[4] G. Wilcher, The use of multiple exostoses in the identification of incinerated human remains, Med. Sci. Law 48 (1) (2008) 82–86.
[5] R.W. Byard, R.A. James, J.D. Gilbert, Diagnostic problems associated with cadaveric trauma from animal activity, Am. J. Forensic Med. Pathol. 23 (3) (2002) 238–244.
[6] G.N. Rutty, C. Robinson, B. Morgan, S. Black, C. Adams, P. Webster, Fimag: the United Kingdom disaster victim/forensic identification imaging system, J. Forensic Sci. 54 (6) (2009) 1438–1442.
[7] G.N. Rutty, C.E. Robinson, R. BouHaidar, A.J. Jeffery, B. Morgan, The role of mobile computed tomography in mass fatality incidents, J. Forensic Sci. 52 (6) (2007) 1343–1349.
[8] E.R. Frykberg, Medical management of disasters and mass casualties from terrorist bombings: how can we cope? J. Trauma Acute Care Surg. 53 (2) (2002) 201–212.
[9] B.G. Brogdon, H. Vogel, J.D. McDowell, A Radiologic Atlas of Abuse, Torture, Terrorism, and Inflicted Trauma, CRC Press, 2003.
[10] M.J. Thali, B. Brogdon, M.D. Viner, Forensic Radiology, CRC Press, 2002.
[11] M.G. Farrell, Daubert v. Merrell Dow Pharmaceuticals, Inc.: epistemilogy and legal process, Cardozo Law Rev. (1993) 2183.
[12] N.R. Council, Strengthening Forensic Science in the United States: A Path Forward, National Academies Press, 2009.
[13] M.J. Bolliger, U. Buck, M.J. Thali, S.A. Bolliger, Reconstruction and 3D visualisation based on objective real 3D based documentation, Forensic Sci. Med. Pathol. 8 (3) (2012) 208–217.
[14] T.D. Ruder, Y. Thali, S.A. Bolliger, S. Somaini-Mathier, M.J. Thali, G.M. Hatch, S.T. Schindera, Material differentiation in forensic radiology with single-source dual-energy computed tomography, Forensic Sci. Med. Pathol. 9 (2) (2013) 163–169.
[15] U. Buck, S. Naether, M. Braun, S. Bolliger, H. Friederich, C. Jackowski, E. Aghayev, A. Christe, P. Vock, R. Dirnhofer, Application of 3D documentation and geometric reconstruction methods in traffic accident analysis: with high resolution surface scanning, radiological MSCT/MRI scanning and real data based animation, Forensic Sci. Int. 170 (1) (2007) 20–28.
[16] D.I. Kim, U. Lee, S.O. Park, D.S. Kwak, S.H. Han, Identification using frontal sinus by three-dimensional reconstruction from computed tomography, J. Forensic Sci. 58 (1) (2013) 5–12.
[17] K.J. Reichs, Quantified comparison of frontal sinus patterns by means of computed tomography, Forensic Sci. Int. 61 (2–3) (1993) 141–168.
[18] A.M. Christensen, Testing the reliability of frontal sinuses in positive identification, J. Forensic Sci. 50 (1) (2005) JFS2004145-5.
[19] L. Atkins, M.S. Potsaid, Roentgenographic identification of human remains, JAMA 240 (21) (1978) 2307–2308.
[20] R.F. da Silva, F.B. Prado, I.G.C. Caputo, K.L. Devito, T. de Luscena Botelho, E.D. Júnior, The forensic importance of frontal sinus radiographs, J. Forensic Leg. Med. 16 (1) (2009) 18–23.
[21] M. Pfaeffli, P. Vock, R. Dirnhofer, M. Braun, S.A. Bolliger, M.J. Thali, Post-mortem radiological CT identification based on classical ante-mortem X-ray examinations, Forensic Sci. Int. 171 (2) (2007) 111–117.
[22] T.L. Beaini, E.F. Duailibi-Neto, I. Chilvarquer, R.F. Melani, Human identification through frontal sinus 3D superimposition: pilot study with cone beam computer tomography, J. Forensic Leg. Med. 36 (2015) 63–69.
[23] M. Iino, H. Fujimoto, M. Yoshida, H. Matsumoto, M.Q. Fujita, Identification of a jawless skull by superimposing post-mortem and ante-mortem CT, J. Forensic Radiol. Imaging 6 (2016) 31–37.
[24] C.M. Bowers, Forensic Dental Evidence: An Investigator's Handbook, Academic Press, 2004.
[25] S. Rhine, K. Sperry, Radiographic identification by mastoid sinus and arterial pattern, J. Forensic Sci. 36 (1) (1991) 272–279.
[26] W. Murphy, F. Spruill, G. Gantner, Radiologic identification of unknown human remains, J. Forensic Sci. 25 (4) (1980) 727–735.
[27] M.P. Rhode, W.W. Goodhue, C.N. Stephan, Radiographic comparison of a fractured clavicle exhibiting a pseudo-arthrosis, J. Forensic Sci. 57 (4) (2012) 1094–1097.
[28] C.N. Stephan, P. Guyomarc'h, Quantification of perspective-induced shape change of clavicles at radiography and 3D scanning to assist human identification, J. Forensic Sci. 59 (2) (2014) 447–453.
[29] W. Martel, J.D. Wicks, R.C. Hendrix, The accuracy of radiologic identification of humans using skeletal landmarks: a contribution to forensic pathology 1, Radiology 124 (3) (1977) 681–684.
[30] D. Rouge, N. Telmon, P. Arrue, G. Larrouy, L. Arbus, Radiographic identification of human remains through deformities and anomalies of post-cranial bones: a report of two cases, J. Forensic Sci. 38 (4) (1993) 997–1007.
[31] S. Tsunenari, K. Yonemitsu, Y. Uchimura, S. Oshiro, Unusual personal identification with characteristic features in chest roentgenograms, Am. J. Forensic Med. Pathol. 3 (4) (1982) 357–360.
[32] B. Hulewicz, G.W. Wilcher, The use of thoracolumbar and hip joint dysmorphism in identification, J. Forensic Sci. 48 (4) (2003) 842–847.
[33] C. Beggan, M. Towers, M. Farrell, K. Jaber, Spinal diastematomyelia: a means of identification of charred remains, J. Forensic Leg. Med. 21 (2014) 5–8.
[34] A.K. Jain, H. Chen, Matching of dental X-ray images for human identification, Pattern Recognit. 37 (7) (2004) 1519–1532.
[35] M. Mahmud, D. Joannic, M. Roy, A. Isheil, J.-F. Fontaine, 3D part inspection path planning of a laser scanner with control on the uncertainty, Comput. Aided Des. 43 (4) (2011) 345–355.
[36] S. Gerbino, D.M. Del Giudice, G. Staiano, A. Lanzotti, M. Martorelli, On the influence of scanning factors on the laser scanner-based 3D inspection process, Int. J. Adv. Manuf. Technol. 84 (9–12) (2016) 1787–1799.
[37] X. Liang, I. Lambrichts, Y. Sun, K. Denis, B. Hassan, L. Li, R. Pauwels, R. Jacobs, A comparative evaluation of cone beam computed tomography (CBCT) and multi-slice CT (MSCT). Part II: on 3D model accuracy, Eur. J. Radiol. 75 (2) (2010) 270–274.
[38] N. Sindhwani, A. Feola, F. De Keyzer, F. Claus, G. Callewaert, I. Urbankova, S. Ourselin, J. D'hooge, J. Deprest, Three-dimensional analysis of implanted magnetic-resonance-visible meshes, Int. Urogynecol. J. 26 (10) (2015) 1459–1465.
[39] J.M. Ford, S.J. Decker, Computed tomography slice thickness and its effects on three-dimensional reconstruction of anatomical structures, J. Forensic Radiol. Imaging 4 (2016) 43–46.
[40] B. Whyms, H. Vorperian, L. Gentry, E. Schimek, E. Bersu, M. Chung, The effect of CT scanner parameters and 3D volume rendering techniques on the accuracy of linear, angular, and volumetric measurements of the mandible, Oral Surg. Oral Med. Oral Pathol. Oral Radiol. 115 (5) (2013) 682.
[41] M. van Eijnatten, F.H. Berger, P. de Graaf, J. Koivisto, T. Forouzanfar, J. Wolff, Influence of CT parameters on STL model accuracy, Rapid Prototyp. J. 23 (4) (2017) 678–685.
[42] F.E. Boas, D. Fleischmann, CT artifacts: causes and reduction techniques, Imaging Med. 4 (2) (2012) 229–240.
[43] N.E. Crow, B.G. Brogdon, The normal lumbosacral spine 1, Radiology 72 (1) (1959) 97.